Model predictive control for comfort optimization in assisted and driverless vehicles

Research Article

Advances in Mechanical Engineering

Advances in Mechanical Engineering
2020, Vol. 12(11) 1–14

DOI: 10.1177/1687814020974532
journals.sagepub.com/home/ade
SAGE

Model predictive control for comfort optimization in assisted and driverless vehicles

Sara Luciani, Angelo Bonfitto, Nicola Amati and Andrea Tonoli

Abstract

This paper presents a method to design a Model Predictive Control to maximize the passengers' comfort in assisted and self-driving vehicles by achieving lateral and longitudinal dynamic. The weighting parameters of the MPC are tuned off-line using a Genetic Algorithm to simultaneously maximize the control performance in the tracking of speed profile, lateral deviation and relative yaw angle and to optimize the comfort perceived by the passengers. To this end, two comfort evaluation indexes extracted by ISO 2631 are used to evaluate the amount of vibration transmitted to the passengers and the probability to experience motion sickness. The effectiveness of the method is demonstrated using simulated experiments conducted on a subcompact crossover vehicle. The control tracking performance produces errors lower than 0.1 m for lateral deviation, 0.5° for relative yaw angle and 1.5 km/h for the vehicle speed. The comfort maximization results in a low percentage of people who may experience nausea (below 5%) and in a low value of equivalent acceleration perceived by the passenger (below 0.315 m/s^2 "not uncomfortable" by ISO 2631). The robustness at variations of vehicle parameters, namely vehicle mass, front and rear cornering stiffness and mass distribution, is evaluated through a sensitivity analysis.

Keywords

Control engineering, automotive control, vehicle engineering, vehicle dynamics, system modeling

Date received: 28 July 2020; accepted: 27 October 2020

Handling Editor: James Baldwin

Introduction

A primary current focus in the automotive industry is the development of advanced solutions exploiting electronic and electromechanical devices for sensing, actuation and control tasks, intending to improve performance, safety and sustainability.[1]

Many of these techniques, known as Advanced Driver Assistance Systems (ADAS), are designed to help the driver controlling the vehicle and are entitled to intervene in case of dangerous maneuvers, driver distraction and high-risk situations. These systems warn, signal and, in some cases, may intervene to mitigate the effect of potential distraction errors of drivers, which are the cause of 40.8% of car accidents.[2] Over the last years, these systems have been gradually introduced in vehicles in parallel with the rising level of driving automation, that is currently settled at the third level of Society of Automotive Engineering (SAE) definition.[3] The affirmation of ADAS and the progressive introduction of autonomous cars on the road aim to change the driving experience. It is predicted to improve many aspects, such as the efficiency of steering, throttle and braking action and, in general, safety. Considerable

Department of Mechanical and Aerospace Engineering, Politecnico di Torino, Torino, Italy

Corresponding author:
Sara Luciani, Department of Mechanical and Aerospace Engineering, Politecnico di Torino, Corso Duca degli Abruzzi 24, I-10129 Torino, Italy.
Email: sara.luciani@polito.it; http://www.lim.polito.it

works have been done to develop reliable and performing control strategies to improve the lateral and longitudinal behavior of the vehicle in every driving condition.[4] Some control strategies are based on a geometric definition of the vehicle model and are mostly used for steering control due to the simplicity of the approach.[5,6] However, they are not suitable for passenger vehicles since the dynamic is not negligible. A possible alternative is represented by dynamic controllers which rely on a dynamic definition of the reference model, as the Model Reference Adaptive Control (MRAC).[7,8] The well-known PID strategy is often used to control either the longitudinal or the lateral dynamic.[9,10] However, these proposed approaches are tested in a particular scenario and the speed does not exceed 35 km/h. A fuzzy sliding mode control is proposed for the vehicle steering actuation at constant speed in Dai and Lee[11] while a neural network is used to adjust the control gain as well as realize the variable gain sliding mode control in Wan et al.[12] Model-based controllers may be applied in combination with PID, like in Levinson et al.,[13] Marcano et al.,[14] and Feraco et al.,[15] where longitudinal and lateral guidance are simultaneously achieved using a Model Predictive Control (MPC) and a PID. MPC is mostly applied in assisted and automated vehicles since it can handle effectively Multi-Input Multi-Output (MIMO) systems with input and state constraints. The formulation could consider non-linear vehicle model,[1,16] as well as linearization of the model around the working point, as presented in Carvalho et al.[17] The vehicle state estimation can also be addressed in the formulation of an MPC, like in Yu et al.[18] where an unscented Kalman filter is used.

Although extensive, the literature related to control strategies for performance and safety improvement for assisted and automated vehicle does not address exhaustively the optimization of the passengers' comfort. Some works make a retrospective evaluation, like in Ren et al.[19] where different control strategies are analyzed and their effectiveness is assessed through three indexes, one of them is the ride comfort index. Although comfort criteria (such as the ones based on ISO 2631 or on the maximum allowable jerk and acceleration) are well known in common practice,[20] to the best of the authors' knowledge, a few control design techniques focusing on comfort optimization are present in the literature. A cascade steering control strategy for autonomous ground vehicles to prevent the velocity from exceeding a specific comfort region is presented in Whitsitt and Sprinkle[21] where a preliminary collection of data is necessary to define the comfort region appropriately. An alternative approach is presented in Mohseni et al.,[22] where an optimal control problem is defined to reduce fuel consumptions and improve the passenger comfort, by minimizing accelerations and jerk. Although the formulation is encouraging, the application of this method is limited to cooperative in standard traffic scenarios. The adoption of weighted root mean square acceleration (WRMSA) as a comfort index, is proposed in Du et al.[23] and Eriksson and Svensson.[24] Different velocity control strategies are presented in Du et al.[23] Each strategy is designed to guarantee the comfort in a particular driving phase, and it should be selected on the basis of the driving condition, limiting the generality of the method. On the other hand, a lateral path planner is hand-tuned using the WRMSA index in Eriksson and Svensson.[24]

The objective of this paper is to propose a method for the design of a control strategy that optimizes the comfort perceived by the passengers and is effective in the tracking control performance. The method is conceived to be applied in assisted and autonomous vehicles and exploits an MPC-based architecture. The proposal is different from previous literature works because it aims to be effective in a wide range of driving conditions, it includes both lateral and longitudinal dynamics, it proposes an off-line method for the weighting parameters of the MPC that has never been presented in previous works. The control is designed for a subcompact crossover SUV. The model embedded in the MPC is a two degrees of freedom (DOF). The cost function of the MPC is designed to guarantee stability of the vehicle, the tracking of the speed profile and minimization of the acceleration along the three axes transmitted to the passengers. This function exploits three coefficients to weight the speed tracking error, lateral deviation and relative yaw angle. These weights are designed offline by means of a Genetic Algorithm (GA) that selects the optimal parameters by minimizing a fitness function that is expressed as the inverse of an equivalent acceleration coefficient, provided by the standard ISO 2631 ("Mechanical vibration and shock – Evaluation of human exposure to whole-body vibration").[25]

The method is tested with simulation experiments conducted in Matlab/Simulink environment using a 14 DOFs vehicle model. The tests are performed using a highway and extra-urban scenarios considering the legal speed limits. The performance of the proposed method is evaluated considering the requirements of the ISO 2631 in terms of equivalent acceleration coefficient and Motion Sickness Dose Value (MSDV). A sensitivity analysis is performed to study the behavior of the control when varying the load of the vehicle, front and rear cornering stiffness and load distribution. Further validation of the effectiveness of the approach is conducted comparing the presented MPC based method with a decoupled control strategy exploiting the combination of an MPC and a PID for the lateral and longitudinal control, respectively. The controller parameters of this second approach have been designed using the

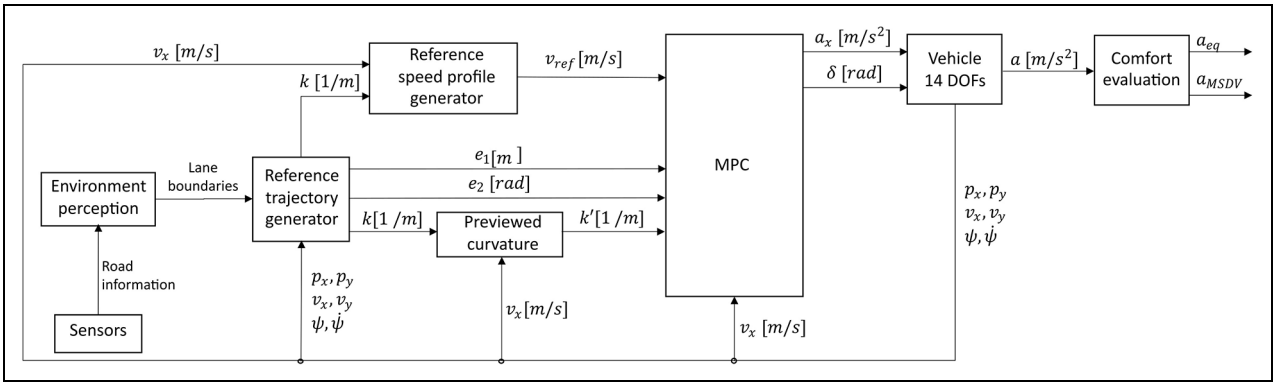

Figure 1. Layout of the proposed method.

same genetic algorithm approach to guarantee the same design methodology as for the proposed MPC method. The obtained results demonstrate the validity of the approach, which resulted in a "not uncomfortable" evaluation according to the ISO equivalent acceleration and a probability of experiencing nausea and sickness lower than 3.5%.

The novel contributions of this paper are: (a) the design of a vehicle dynamic control that maximizes the comfort perceived by the passengers by respecting the tracking control requirements along lateral and longitudinal directions; (b) a method for the off-line tuning of the MPC weighting parameters by means of a Genetic algorithm whose cost function is based on comfort index evaluation extracted from ISO 2631.

The paper presents the method in Section 2 where vehicle modeling, definition of the comfort evaluation indexes, control design and MPC weighting parameter selection are discussed. The results are presented in Section 3 in the following three analyzes: (a) control tracking and comfort performance evaluation, (b) comparison with a decoupled MPC and PID control strategy, and (c) control robustness analysis when varying vehicle parameters.

Method

The layout of the proposed method is illustrated in Figure 1. The environment perception task receives as input the data from the sensors installed on the vehicle namely cameras, lidars, GPS. The fusion of this data provides information about the environment surrounding the vehicle. Specifically, the lane boundaries, the presence of obstacles and traffic signs are detected. Owing to this information and the real time measurements of the vehicle states, a reference trajectory and a speed profile are computed.

In this work, the reference trajectory corresponds to the center line of the lane and it is computed as the average between the right boundary of the lane and the left one. The reference speed profile to follow the generated trajectory is based on two different criteria. The first one is related to the geometry of the road while the second one limits the lateral acceleration. Thus, the vehicle's reference velocity is imposed equal to the minimum value between the maximum velocity imposed by the road geometry and the velocity computed limiting the lateral acceleration. Afterwards, MPC provides the wheel steering angle and the acceleration/deceleration command to ensure the automated vehicle guidance along the generated trajectory. The controller parameters (Q_{11}, Q_{22}, Q_{33}) are tuned off-line by means of a Genetic algorithm that is used to minimize the equivalent acceleration a_{eq} on the basis of the vehicle accelerations.

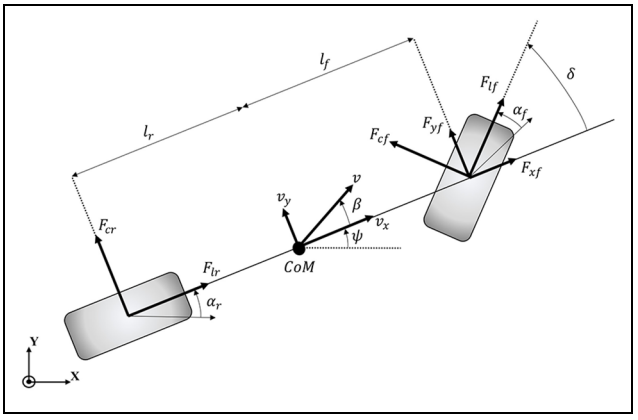

Figure 2. Bicycle vehicle model.

Vehicle modeling

In this section, the vehicle model embedded in the MPC and the verification model used for the validation of the method are illustrated.

Reference model for MPC. The reference model for MPC is based on a bicycle representation of the vehicle.[26] Referring to Figure 2, x and y are the coordinates of

the center of mass (CoM) in an inertial reference frame (X, Y), ψ is the heading angle and $\dot{x}$ and $\dot{y}$ are the longitudinal and lateral velocities respectively, l_f and l_r represent the distance of CoM from the front and rear axles respectively, β is the angle between the CoM current velocity V and the longitudinal axis of the vehicle.

When lateral dynamic is considered, the equations of motion are computed applying the second Euler equation along y axis and the moment balance along z axis.

$$ma_y = -mv_x\dot{\psi} + F_{yf} + F_{yr} \tag{1}$$

$$I_{zz}\ddot{\psi} = l_f F_{yf} - l_r F_{yr} \tag{2}$$

where F_{yf} and F_{xr} denote lateral forces applied respectively to front and rear wheels, along vehicle- fixed y axis. The lateral tire force is proportional to the slip angle of the tire

$$F_{yf} = 2C_{\alpha f}\left(\delta - \theta_{V_f}\right) = 2C_{\alpha f}\alpha_f \tag{3}$$

$$F_{yr} = 2C_{\alpha r}\left(-\theta_{V_r}\right) = 2C_{\alpha r}\alpha_r \tag{4}$$

where $C_{\alpha f}$ and $C_{\alpha r}$ denote the cornering stiffness of front and rear tires. To compute θ_{V_f} and θ_{V_r}, the following relations can be used:

$$\tan\left(\theta_{V_f}\right) = \frac{v_y + l_f\dot{\psi}}{v_x} \tag{5}$$

$$\tan\left(\theta_{V_r}\right) = \frac{v_y + l_r\dot{\psi}}{v_x} \tag{6}$$

In the MPC formulation, a linearized vehicle model is considered. If the assumption of small angles is verified, the following approximation is valid

$$\theta_{V_f} = \frac{v_y + l_f\dot{\psi}}{v_x} \tag{7}$$

$$\theta_{V_r} = \frac{v_y + l_r\dot{\psi}}{v_x} \tag{8}$$

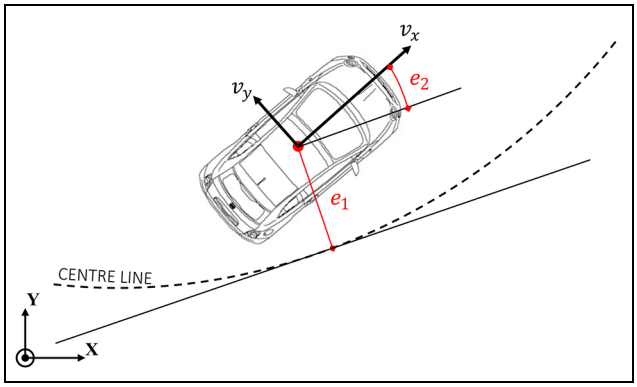

Figure 3. Vehicle model in terms of lateral deviation e_1 and relative yaw angle e_2.

To define explicitly the controlled variable, the equations (1) and (2) are organized in terms of errors with respect to the road, lateral deviation, and relative yaw angle. As shown in Figure 3, the lateral deviation e_1 is defined as the distance between the center of mass of the vehicle and the closest point on the desired path while the relative yaw angle e_2 indicates the angle between the vehicle's center line and the tangent at the desired path. If small relative yaw angle and constant curvature κ are assumed,

$$\dot{e}_1 = v_y + v_x e_2 \tag{9}$$

$$e_2 = \psi - \psi_{des} \tag{10}$$

where

$$\dot{\psi}_{des} = v_x\kappa \tag{11}$$

The longitudinal dynamics is implemented through a first order transfer function that incorporates a lag in tracking desired acceleration.[26]

$$a_x = \frac{1}{\tau s + 1}a_{x,\,des} \tag{12}$$

The resulting state space representation of the model embedded in the MPC is

$$\begin{bmatrix} \ddot{v}_x \\ \dot{v}_x \\ \dot{v}_y \\ \ddot{\psi} \\ \dot{e}_1 \\ \dot{e}_2 \end{bmatrix} = \begin{bmatrix} -\frac{1}{\tau} & 0 & 0 & 0 & 0 & 0 \\ 1 & 0 & 0 & 0 & 0 & 0 \\ 0 & 0 & -\frac{2C_f + 2C_r}{mv_x} & -V_x - \frac{2C_{\alpha f}l_f - 2C_{\alpha r}l_r}{mv_x} & 0 & 0 \\ 0 & 0 & -\frac{2C_{\alpha f}l_f - 2C_{\alpha r}l_r}{I_z v_x} & -\frac{2C_{\alpha f}l_f^2 + 2C_{\alpha r}l_r^2}{I_z v_x} & 0 & 0 \\ 0 & 0 & 1 & 0 & 0 & V_x \\ 0 & -\kappa & 0 & 1 & 0 & 0 \end{bmatrix} \begin{bmatrix} \dot{v}_x \\ v_x \\ v_y \\ \dot{\psi} \\ e_1 \\ e_2 \end{bmatrix} + \begin{bmatrix} \frac{1}{\tau} & 0 \\ 0 & 0 \\ 0 & \frac{2C_{\alpha f}}{m} \\ 0 & \frac{2l_f C_{\alpha f}}{I_z} \\ 0 & 0 \\ 0 & 0 \end{bmatrix} \begin{bmatrix} \dot{v}_x \\ \delta \end{bmatrix} \tag{13}$$

The main parameters of the subcompact crossover SUV considered in this study are reported in Table 1.

Table 1. Main parameters of the considered vehicle.

Parameter	Symbol	Value	Unit
Mass	m	1270	$[kg]$
Inertia	I_{zz}	1550	$[kg \cdot m^2]$
Distance from CoM to front/rear axle	l_f/l_r	1.02/1.9	$[m]$
Front/Rear cornering stiffness	$C_{\alpha f}/C_{\alpha r}$	65765/49517	$[N/rad]$

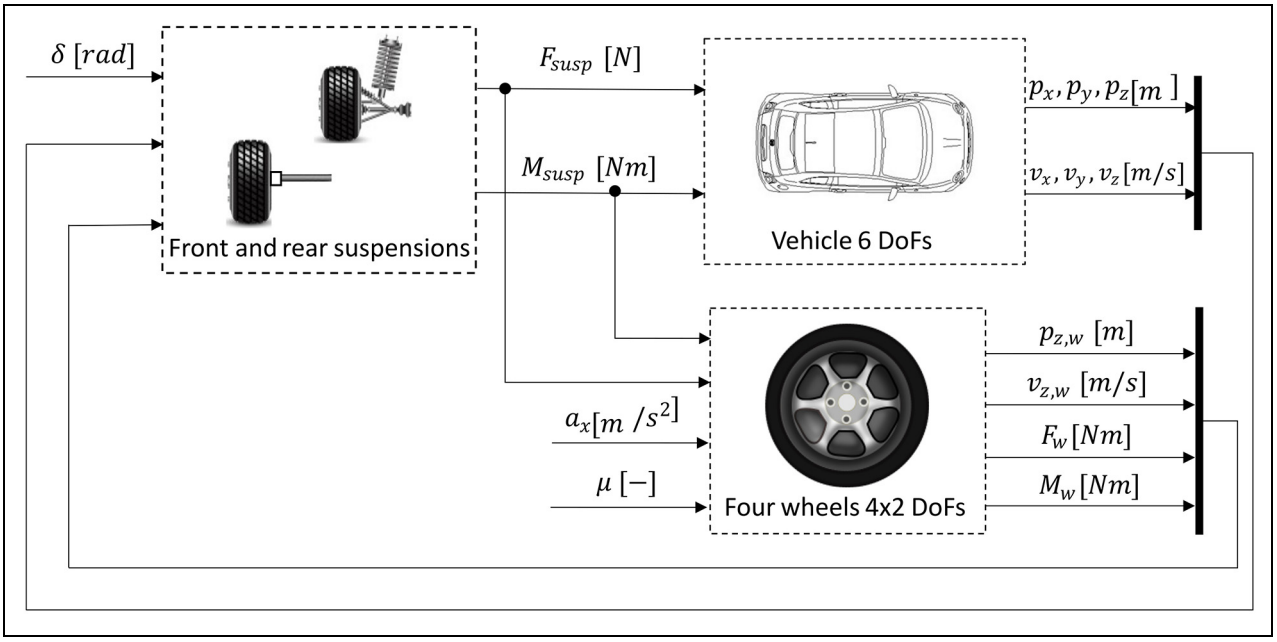

Figure 4. Block scheme of the 14 DOFs vehicle model.

Verification model. The verification model consists of a 14 DOFs vehicle model implemented in Simulink. A six degrees of freedom rigid two-axle vehicle body is used to represent the longitudinal, lateral, vertical, pitch, roll and yaw motions. The model considers body mass, inertia, weight distribution between the axles due to suspension and suspension forces and moments. A two degrees of freedom wheel model is applied. It implements the vertical and lateral behavior of a wheel adopting the Pacejka Magic Formula. To simplify the analysis, lumped unsprung and sprung masses are used, the steer angle of the left and right wheels is assumed to be the same and the tires are assumed to be always in contact with the ground.[26] Figure 4 represents the block scheme of 14 DOFs model. The inputs of the plant are the wheel steering angle (δ), the longitudinal acceleration a_x and the friction coefficient μ. The suspension block implements an independent mapped front suspension and a mapped solid axle rear suspension. Assuming massless suspensions, the suspension forces and moments applied to the vehicle are equal to the suspension forces and moments applied to the wheel. The suspension forces and moments (F_{susp}, M_{susp}) are the inputs of the vehicle and wheels blocks. Afterwards, the vehicle block feedbacks the front and rear axles displacements and velocities while the wheel block computes the vehicle forces, the moments applied to the vehicle along fixed axes (F_w, M_w) and the displacement and velocity of the wheel along z-axis ($p_{z,w}, v_{z,w}$).

Definition of comfort evaluation indexes

In the recent past, comfort evaluation was addressed considering mainly ergonomic factors such as seat vibrations and noise. The introduction of assisted and autonomous vehicles suggested to include additional indexes related to natural movements, motion sickness, disturbances and apparent safety in the analysis.[27]

Qualitative definitions of comfort and ride quality are provided by ISO 5805, which defines comfort as a "*subjective state of well-being or absence of mechanical disturbance in relation to the induced environment (mechanical vibration or repetitive shock)*," and ride quality as a "*degree to which the whole subjective*

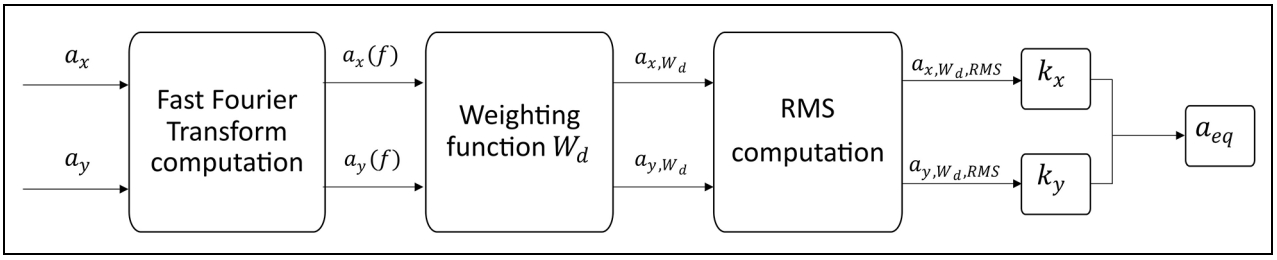

Figure 5. Procedure to calculate the equivalent acceleration.

experience (including the motion environment and associated factors) of a journey is perceived and rated as favourable or unfavourable by passengers or operators." The comfort is thus influenced by environment physical factors and individual sensitivity to them while the ride quality is a metric describing a person's subjective perception of a vehicle ride.

On the other hand, a quantitative evaluation of the comfort can be conducted based on ISO 2631 which defines metrics to quantify the whole-body vibration in relation to human health and comfort, probability of vibration perception and incidence of motion sickness.

In this study two indexes extracted from ISO 2631 have been considered. The first one (a_{eq}) considers an equivalent acceleration along the x and y axes while the second one ($MSDV$) studies the probability to experience motion sickness.

The computation of the first index is obtained as indicated in Figure 5.

A Fast Fourier Transform (FFT) is applied to the longitudinal and lateral accelerations a_x and a_Y. The resulting accelerations in frequency domain are multiplied by a weighting function W_d (illustrated in dashed line in Figure 6) and afterwards the root mean square (RMS) is computed. The resulting frequency weighted root mean square (WRMS) along the main axes is

$$a_{W_{i,RMS}} = \left(\frac{1}{T}\int_{t_0}^{t_f} a_{W_i}^2(t)dt\right)^{\frac{1}{2}} \tag{14}$$

where T_f is the integration time, a_{W_i} the instantaneous frequency weighted acceleration, W_i frequency weighted function, and $a_{W_{i,RMS}}$ the root mean square of a_{W_i}.

The equivalent acceleration index is then calculated multiplying the frequency-WRMS acceleration components by squared axis coefficients (k_x, k_y) which are depending on the type of transportation and are specified by the ISO.

$$a_{eq} = (k_x^2 a_{x,W}^2 + k_y^2 a_{y,W}^2)^{\frac{1}{2}} \tag{15}$$

where $a_{x,W}$, $a_{y,W}$ are the weighting RMS accelerations with respect to the orthogonal x, y axes respectively.

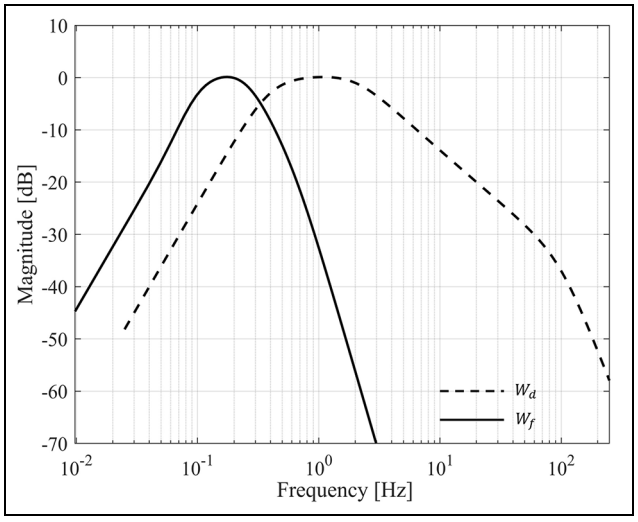

Figure 6. Amplitude response of the weighting function W_d(dashed line) in ISO 2631-1 and W_f (solid line) in MSDV.

Table 2. Likely reactions to various magnitudes of overall vibration total values, specified in ISO 2631-1.

$a_{eq} \leqslant 0.315 m/s^2$	Not uncomfortable
$0.315 m/s^2 \leqslant a_{eq} \leqslant 0.63 m/s^2$	A little uncomfortable
$0.5 m/s^2 \leqslant a_{eq} \leqslant 1 m/s^2$	Fairly uncomfortable
$0.8 m/s^2 \leqslant a_{eq} \leqslant 1.6 m/s^2$	Uncomfortable
$1.25 m/s^2 \leqslant a_{eq} \leqslant 2.5 m/s^2$	Very uncomfortable
$a_{eq} \geqslant 2 m/s^2$	Extremely uncomfortable

The longitudinal and lateral coefficients k_x and k_y are equal to 1.

The evaluation of the comfort based on the equivalent acceleration index a_{eq} is obtained approximate reactions at various magnitudes of the index provided by the ISO 2631 and presented in Table 2.

The second index aims to evaluate the probability of the motion sickness occurrence as an effect of the oscillatory motion. As a matter of fact, motion at frequencies lower than $0.5Hz$ can produce motion sickness in the passengers and the likelihood of nausea symptoms increases with increasing duration of motion exposure. The index Motion sickness dose value (MSDV) is

proposed by the standard to measure the probability of this occurrence and it is computed with the same method as the first index a_{eq} illustrated in Figure 5. The resulting index is:

$$a_{MSDV} = \left(\int_{t_0}^{T_f} \left[a_{W_f}(t) \right]^2 dt \right)^{\frac{1}{2}} \tag{16}$$

where T_f is the full period of exposure, a_{W_i} the instantaneous frequency weighted acceleration, W_f is the a frequency weighted function showed in solid line in Figure 6. Although people reactions to low frequency motion are linked to the personal susceptibility, ISO 2631 indicates that the percentage who may vomit is approximately given by

$$a_{MSDV}[\%] = K_m \cdot a_{MSDV} \tag{17}$$

where K_m is equal to 1/3.

MPC design

A MPC is adopted to control the lateral and longitudinal dynamics of the vehicle. As illustrated in Figure 1, the architecture of the control strategy is composed of an optimizer, performing the on-line optimization, and an embedded reference vehicle model (equation (13)), used to obtain the optimal actions for the control measures. The inputs to the MPC are: (1) the previewed curvature κ', which is the sequence of the upcoming road curvature values, (2) lateral deviation e_1, (3) relative yaw angle e_2, and (4) the reference velocity V_{ref}. The output of the MPC is the front-wheel steering angle δ and the desired longitudinal acceleration to track a specific path a_x. Based on the reference velocity, the MPC computes the desired acceleration to track the velocity and, minimizing the lateral deviation e_1 and the relative yaw angle e_2, the steering command is provided to the vehicle to maintain the center line and follow the trajectory.

Given the control sampling interval T_s, that is the command output ratio, at each time step k (corresponding to the time instant $t = kT_s$) the controller receives the current states $x(k)$ of the vehicle and solves an open-loop optimal control problem to determine the optimal commands $u(k), ..., u(k + H_c - 1)$, where H_c is the control horizon. The optimization relies on a prediction of the behavior of the vehicle over an interval $[k, k + H_p]$, where H_p is called the prediction horizon that is based on the embedded reference vehicle model. The generation of the control commands derives from the optimization of a cost function $J(k)$ over the prediction period $[k, k + H_p]$, subject to the operational constraints. When the optimal values are found by the controller, only the first control action of the optimal control sequence is applied to the system. Then, the prediction horizon is shifted one step forward and, over the shifted horizon, the prediction and optimization procedure are repeated using new system measurements. Thus, the optimization problem to be solved at each time step is:

$$\begin{aligned}
\min_u J = & \sum_{j=1}^{N_y} \sum_{i=1}^{H_p} \left\| y_j(k+i|k) - y_{j,ref}(k+i|k) \right\|_{Q_y} \\
& + \sum_{j=1}^{N_u} \sum_{i=0}^{H_p-1} \left\| u_j(k+i|k) - u_j(k+i-1|k) \right\|_{R_u} \\
& subject\ to\ x(k+j+1|k) = Ax(k+j|k) \\
& \quad + B_u u(k+j|k) + B_d v(k+j|k) \\
& x(k|k) = x(k) \\
& y(k+j|k) = Cx(k+j|k) \\
& |u(k+j|k) \leqslant u_{limit}
\end{aligned} \tag{18}$$

where u is the control command, $y_j(k + i|k)$ is the predicted value of the j-th output plant at the i-th prediction horizon step, $y_{j,ref}(k + i|k)$ is the reference value for the j-th output plant at the i-th prediction horizon step. The weighted norm of the vector $y = [y_1, y_2, y_3]$ and $u = [u_1, u_2]$ are equal to:

$$\left\| y_j(k+i|k) - y_{j,ref}(k+i|k) \right\|_{Q_y} = y(k+i|k)^T Q_y y(k+i|k)$$

$$\left\| u_j(k+i|k) - u_j(k+i-1|k) \right\|_{R_u} = u_j(k+i|k)^T R_u u_j(k+i-1|k)$$

$Q_y = diag([Q_{11}, Q_{22}, Q_{33}])$ and $R_u = diag([R_{11}, R_{22}])$ are the design matrices chosen according to the desired performance trade off. Q_{11}, Q_{22}, and Q_{33} are the weighting parameters for the velocity, lateral deviation and relative yaw angle respectively. Afterwards, the optimization problem is solved by a standard quadratic program (QP) solver based on Knows What It Knows (KWIK) algorithm.[28]

Selection of MPC weighting parameters

The achievement of comfort optimization and vehicle control performance relies on the tuning of the weighting parameters of the matrix Q_y. The system requirements that have been considered are:

- tracking velocity error $V_{x,err} \leqslant 2[km/h]$,
- lateral deviation $|e_1| \leqslant 0.10[m]$,
- relative yaw angle $|e_2| \leqslant 2[deg]$.

On the basis of these specifications, the lower and upper bounds of the weighting parameters have been defined:

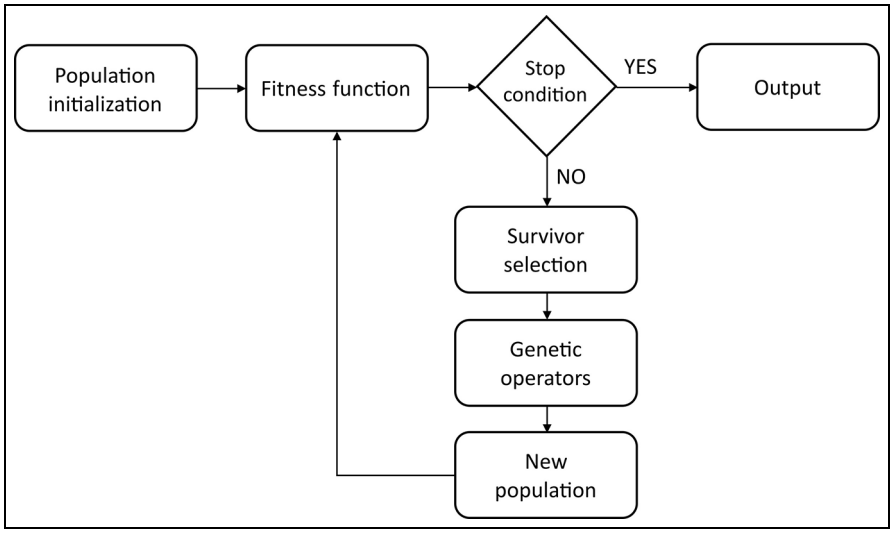

Figure 7. Genetic algorithm working flow.

$$0 < Q_{11} < 100$$
$$0 < Q_{22} < 50$$
$$0 < Q_{33} < 0.5$$

The most suitable set of weighting parameters in terms of comfort optimization have been selected among all the possible combinations of Q_{11}, Q_{22}, and Q_{33} by means of a Genetic Algorithm (GA). This method is widely adopted in several engineering problems for identification and optimization tasks.[29,30] It is based on an iterative process of selective reproduction acting on a set of solutions to a given problem. The fittest solution is a global optimum and is the one surviving along the generations. The common working principle of a GA is depicted in Figure 7.

A GA works on a population composed by a certain number of solutions, called chromosomes. The chromosomes are the transliteration of all the parameters of the solution. Each chromosome is made by genes which can be encoded by binary or floating numbers. After the first population is randomly created, each chromosome is compared to the others in the population and evaluated through a fitness functions that indicates how successful the solution is. Higher is the fitness rating, higher the quality of the solution and the possibility to mate and yield more fitter individuals. The following populations are generated to encode better solutions using genetic operators, also known as evolution operators, namely elitism, crossover, and mutation.

In the present study, a population of 20 individuals in 60 generations is considered. The Arithmetic Crossover Procedure and the Uniform Mutation Method are adopted as genetic operators. The selection of the best individuals is performed using a Normalized Geometric selection since the individuals in the population have very close fitness values. This method assigns a probability to each individual based on the rank of solutions after they are sorted. The stop condition is satisfied when the maximum number of generations is reached. In the proposed solution, each chromosome k of the i-th generation is encoded as a vector of real numbers:

$$X_k^i = \left[x_{k,1}^i, x_{k,2}^i, x_{k,3}^i\right] \tag{19}$$

where $[x_{k,1}, x_{k,2}, x_{k,3}] = [Q_{11}, Q_{22}, Q_{33}]$ and assume values included within the ranges above defined. The fitness function F_{obj} is determined to optimize the comfort perceived by the passengers and is equal to

$$F_{obj} = \frac{1}{a_{eq}} \tag{20}$$

where a_{eq} is computed applying equation (2). The index $MSDV$ could be used equivalently instead of a_{eq}. A fitness function combining the two indexes has been tested without benefits. The GA design procedure is the following:

(1) An initial population is randomly generated (20 individuals).
(2) The vehicle simulation is performed, and the acceleration data are collected and post-processed to get a_{eq}.
(3) The fitness value is computed for each chromosome.
(4) The best set of chromosomes are selected implementing the Normalized Genetic selection.

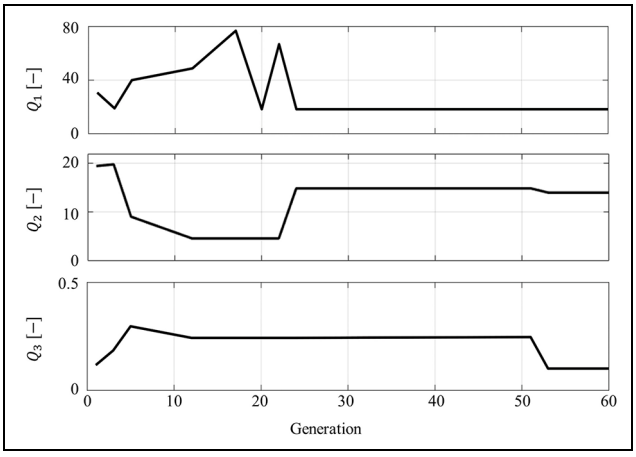

Figure 8. Convergence trends of the best chromosome for the coupled control strategy.

(5) The survivor selection based on elitism is applied to do not lose potential fittest solutions in the next generation.
(6) New individuals are generated applying the Arithmetic Crossover procedure.
(7) To introduce and maintain diversity in the population Uniform Mutation Method is applied.
(8) A new population is created according to F_{obj}. Steps 2–7 are evaluated until the 60-th generation is reached.

The tuning of the parameters has been conducted considering several driving scenarios in the following categories: urban, extra-urban and highway. This design choice allows providing a result that is general with respect to the driving conditions.

Figure 8 and Table 3 shows the graphical and numerical convergence trends of the best chromosome. The identified parameters are $Q_{11} = 18.22, Q_{22} = 14.02$, and $Q_{33} = 0.10$.

Table 3. Fitness function values of the best chromosome among all the generations.

Generation	Q_{11}	Q_{22}	Q_{33}	F_{obj}
1	30.63	19.48	0.12	6.156
3	18.90	19.81	0.18	6.159
5	39.93	9.08	0.30	6.165
12	48.69	4.64	0.24	6.178
17	76.73	4.64	0.24	6.178
20	18.22	4.64	0.24	6.180
22	66.71	4.64	0.24	6.183
24	18.22	14.89	0.24	6.187
51	18.22	14.89	0.25	6.187
53	18.22	14.01	0.10	6.190
60	18.22	14.01	0.10	6.190

Results and discussion

The evaluation of the proposed method effectiveness is conducted in three cases: (a) analysis of control tracking performance and passenger comfort evaluation on a highway and extra-urban scenarios; (b) comparison of the proposed method with an alternative control strategy based on a MPC and PID for the longitudinal and lateral dynamics respectively; and (c) sensitivity analysis of the proposed method when varying the values of mass, cornering stiffness and mass distribution of the vehicle.

MPC performance analysis

The control strategy is tested in a highway and extra-urban scenarios to evaluate the passenger comfort and tracking performance. The road scenarios in XY reference frame and the corresponding curvatures κ are reported in Figure 9. The highway scenario is modeled with three lanes and features a minimum curvature radius of $215[m]$ while the extra-urban scenario has only two lanes and presents lower curvature radius values.

Figure 10 presents the results obtained in the two scenarios: (a) is the highway and (b) is the extra-urban scenario in terms of lateral deviation (subplots a.1 and b.1), comparison between the reference and the actual speed (subplots a.2 and b.2), relative yaw angle (subplots a.3 and b.3), front wheel steering angle (subplots a.5 and b.5), longitudinal acceleration (subplots a.4 and b.4) and lateral acceleration (subplots a.6 and b.6).

In both scenarios, the tracking control performance are satisfied. The longitudinal velocity is tracked with an error that is much smaller than $2[km/h]$ (Figure 10(a.2) and (b.2)), the lateral deviation is always within the range $\pm 0.05[m]$(Figure 10(a.1) and (b.1)) and relative yaw angle variations are smaller than $0.4[deg]$ (Figure 10(a.3) and (b.3)), as expected. The front wheel steering angle δ is always in the range $\pm 1.5[deg]$ (Figure 10(a.5) and (b.5)) while the maximum value of longitudinal acceleration is $3.8[m/s^2]$ in the highway scenario (Figure 10(a.4)). The lateral acceleration reaches its maximum value of $2.9[m/s^2]$ in the extra-urban scenario (Figure 10(b.6)). The passenger comfort is evaluated by means of the two indexes. The equivalent acceleration index a_{eq} is "not uncomfortable" (see Table 2) in both cases. The second index a_{MSDV} reveals that the probability of people who may experience motion sickness is equal to 3.4% and 4.9% for the highway and the extra-urban scenario respectively. This percentage has to be considered as the worst-case condition and are aligned with the expected results.

Comparison with a decoupled strategy based on MPC and PID

An additional validation of the effectiveness of the proposed approach is obtained comparing it with a

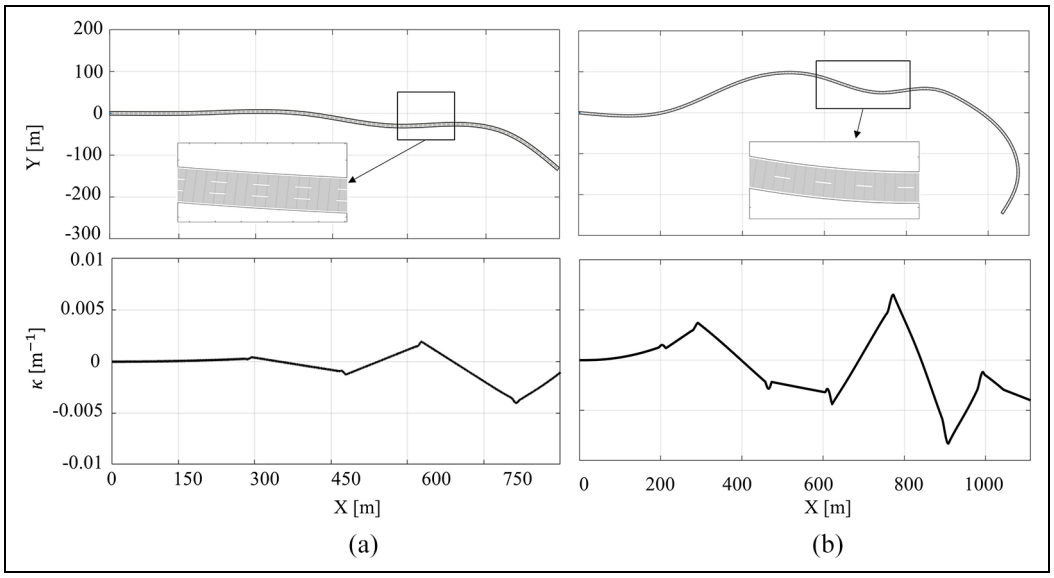

Figure 9. (a) Highway scenario and road curvature $\kappa\left[m^{-1}\right]$ and (b) Extra-urban scenario and road curvature $\kappa\left[m^{-1}\right]$.

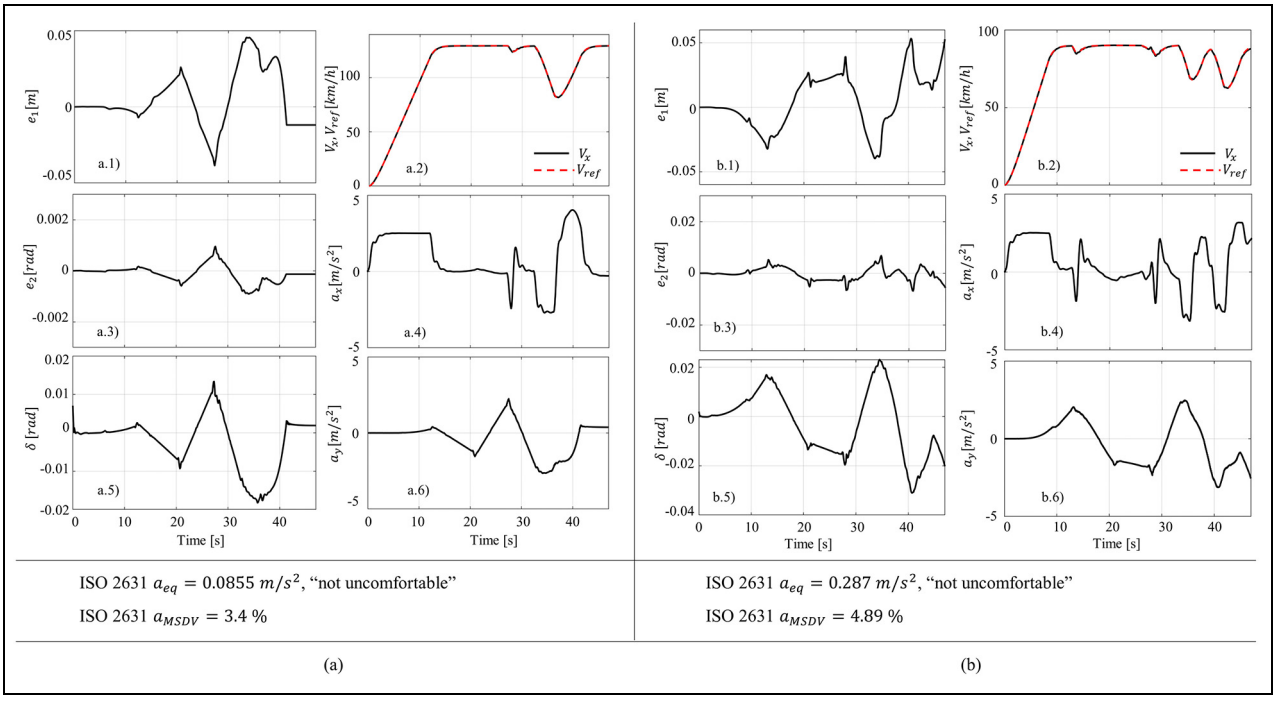

Figure 10. Results obtained in the highway scenario: (a) Highway scenario, (b) Extra-urban scenario, (a.1-b.1) Lateral deviation e_1, (a.2-b.2) Reference velocity V_{ref} (red dashed line) versus Actual longitudinal speed V_x (solid black line), (a.3-b.3) Relative yaw angle e_2, (a.4-b.4) Longitudinal acceleration a_x, (a.5-b.5) Front wheel steering angle δ, and (a.6-b.6) Lateral acceleration a_y.

decoupled control strategy based on a MPC and a PID to control the lateral and the longitudinal dynamics respectively. As shown in Figure 11 which replaces the MPC control block in Figure 1, the inputs to the MPC are: the previewed curvature κ'; lateral deviation e_1; relative yaw angle e_2; and the longitudinal vehicle velocity V_x. The output of the MPC is the front-wheel steering angle δ. On the other hand, the inputs of the PID are the reference velocity V_{ref} and actual vehicle velocity V_x. The PID command is the desired longitudinal acceleration a_x.

Also for this control strategy, a Genetic Algorithm is applied to tune the control parameters on the basis of the comfort index a_{eq}. The applied procedure is the

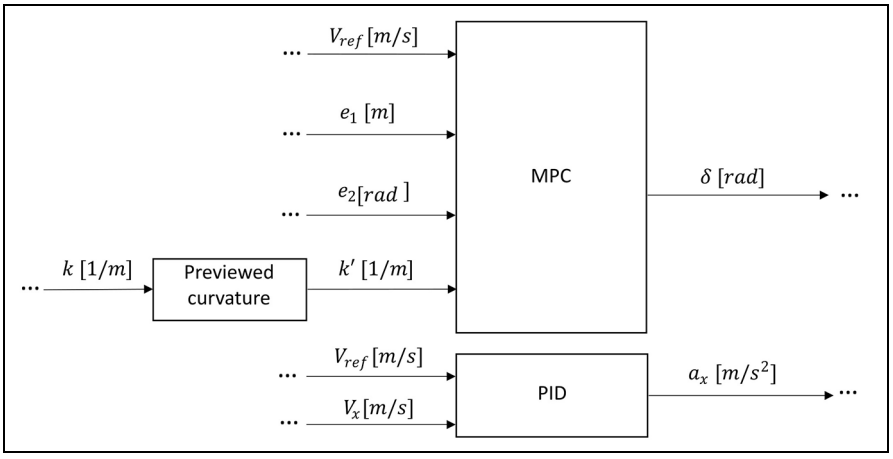

Figure 11. Scheme of MPC and PID control strategy. The two blocks replace the MPC control block in Figure 1.

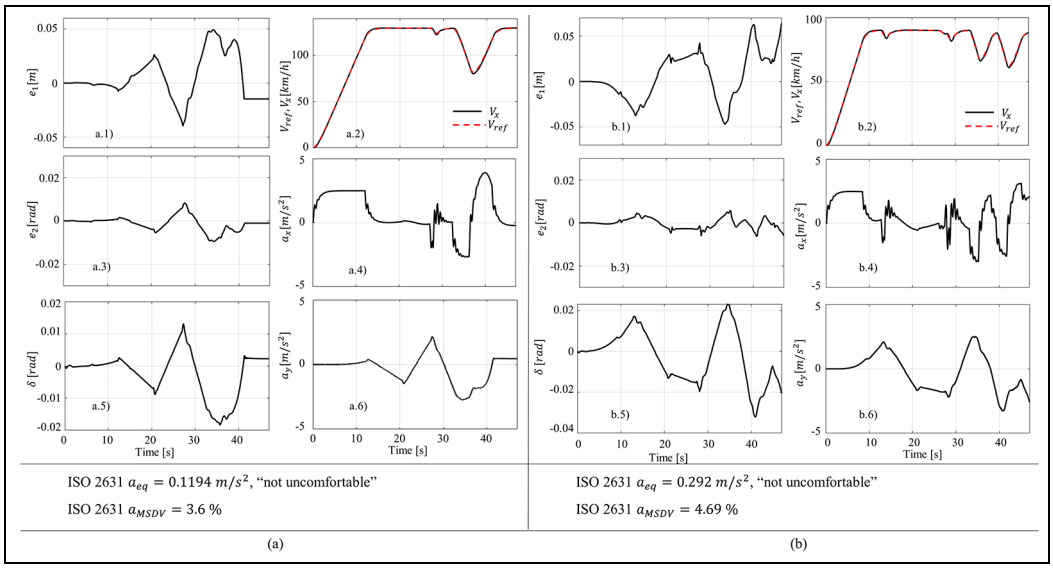

Figure 12. Results obtained in the highway scenario: (a) Highway scenario, (b) Extra-urban scenario, (a.1-b.1) Lateral deviation e_1, (a.2-b.2) Reference velocity V_{ref} (red dashed line) versus Actual longitudinal speed V_x (solid black line), (a.3-b.3) Relative yaw angle e_2, (a.4-b.4) Longitudinal acceleration a_x, (a.5-b.5) Front wheel steering angle δ, and (a.6-b.6) Lateral acceleration a_y.

same as that explained in section "Selection of MPC weighting parameters". In this case, each chromosome is composed of the weighting values of the Q_y matrix in the MPC cost function and the PID parameters:

$$X_k^i = [x_{k,1}^i, x_{k,2}^i, x_{k,3}^i, x_{k,4}^i, x_{k,5}^i] \tag{21}$$

where $[x_{k,1}, x_{k,2}, x_{k,3}, x_{k,4}, x_{k,5}] = [K_p, K_i, K_d, Q_{11}, Q_{22}]$. The identified parameters are $Q_{11} = 95.71, Q_{22} = 0.53$, $K_p = 5.87, K_i = 0.98, K_d = 0.97$.

Afterwards, the controller is tested on the scenarios illustrated in Figure 9. The performance of the decoupled control strategy is shown in Figure 12, that is structured as Figure 10. As expected, the comfort performance is nearly equal to the proposed method since only the longitudinal control has been changed. For this reason, the longitudinal dynamic is less relevant with respect to the lateral for the comfort evaluation. However, good comfort evaluation results are obtained at the expense of lower control tracking performance. The lateral deviation, the relative yaw angle and speed tracking are indeed slightly worse than the single MPC case. In particular, the lateral deviation is in the range $\pm 0.6[m]$ (Figure 12(a.1) and (b.1)) and the relative yaw angle is within $0.5[deg]$. The speed profile (Figure 12(a.2) and (b.2)) is well-tracked while the

Table 4. Vehicle parameters for sensitivity analysis.

Case	Mass $[kg]$		Cornering stiffness [front, rear] $[Nrad^{-1}]$		Mass distribution $[m]$	
	Value	Variation wrt nominal value (Case 0)	Value	Variation wrt nominal value (Case 0)	Value	Variation wrt nominal value (Case 0)
0	1270	0%	[65765, 49517]	0%	[1.02, 1.89]	0%
1	1610	+27%	[65765, 49517]	0%	[1.02, 1.89]	0%
2	1270	0%	[78918, 59420]	+20%	[1.02, 1.89]	0%
3	1270	0%	[52612, 39613]	−20%	[1.02, 1.89]	0%
4	1270	0%	[65765, 49517]	0%	[1.89, 1.02]	[+85%, − 46%]

Table 5. Mean and peaks values of velocity error, lateral deviation, relative yaw angle, wheel steering angle, longitudinal and lateral acceleration for each case of variation.

		$V_{x,err}[km/h]$	$e_1[m]$	$e_2[rad]$	$\delta[rad]$	$a_x[m/s^2]$	$a_y[m/s^2]$
Case 0	Mean value	1.454	$1.61 \cdot 10^{-2}$	$2.50 \cdot 10^{-3}$	$4.90 \cdot 10^{-3}$	1.262	0.776
	Peak value	1.546	$5.37 \cdot 10^{-2}$	$9.5 \cdot 10^{-3}$	$1.82 \cdot 10^{-2}$	3.6	2.5
Case 1	Mean value	1.436	$1.61 \cdot 10^{-2}$	$2.50 \cdot 10^{-3}$	$4.89 \cdot 10^{-3}$	1.263	0.764
	Peak value	1.548	$5.37 \cdot 10^{-2}$	$9.5 \cdot 10^{-3}$	$1.82 \cdot 10^{-2}$	3.61	2.5
Case 2	Mean value	1.440	$1.61 \cdot 10^{-2}$	$2.50 \cdot 10^{-3}$	$4.89 \cdot 10^{-3}$	1.263	0.765
	Peak value	1.551	$5.37 \cdot 10^{-2}$	$9.5 \cdot 10^{-3}$	$1.82 \cdot 10^{-2}$	3.61	2.52
Case 3	Mean value	1.448	$1.61 \cdot 10^{-2}$	$2.50 \cdot 10^{-3}$	$4.89 \cdot 10^{-3}$	1.263	0.765
	Peak value	1.559	$5.37 \cdot 10^{-2}$	$9.5 \cdot 10^{-3}$	$1.82 \cdot 10^{-2}$	3.61	2.51
Case 4	Mean value	2.353	$1.61 \cdot 10^{-2}$	$2.50 \cdot 10^{-3}$	$4.88 \cdot 10^{-3}$	1.262	0.748
	Peak value	2.465	$5.37 \cdot 10^{-2}$	$9.5 \cdot 10^{-3}$	$1.82 \cdot 10^{-2}$	3.6	2.5

maximum longitudinal acceleration increases up to $4.2[m/s^2]$ in the highway scenario (Figure 12(a.4)). The front wheel steering angle as well as the lateral acceleration are almost equal to the ones presented in Figure 10.

Sensitivity analysis

The last analysis is conducted to validate the robustness of the proposed control strategy at variation of four vehicle parameters: mass, front and rear cornering stiffness and mass distribution. The map of the variations of the parameters is illustrated in Table 4. Five different parameter combinations are considered. The setting of the vehicle with the parameters assuming their nominal values is called Case 0. The mass is changed to consider the variation of load, the cornering stiffness is altered to simulate different types of tires and the mass distribution is modified to take into account the variation of the center of mass.

For the five settings, the simulation has been performed on the extra-urban scenario and the mean and peak values of the longitudinal speed error, lateral deviation, relative yaw angle, wheel steering angle, longitudinal and lateral acceleration have been recorded and are reported in Table 5.

This analysis highlights that the control is robust at the variation of the above mentioned four parameters. As it is evident from the table, the main difference is recorded at varying the mass distribution. The velocity mean error increases up to $2.353[km/h]$ while in the other cases it is mostly $1.45[km/h]$. Apart from Case 4, the values of velocity mean error, lateral deviation, relative yaw angle, front wheel steering angle and accelerations confirm a constant trend, and they are almost equal to the ones reported for Case 0. Furthermore, the negligible variations in the values corresponding to the lateral and longitudinal accelerations confirm that the comfort evaluation is not significantly affected. The lateral acceleration decreases by $0.012[m/s^2]$ along with the different cases while the longitudinal acceleration is almost equal to Case 0.

Conclusion

In this paper, an MPC designed to optimize the tracking of speed profile, lateral deviation and relative yaw angle and maximize the passenger comfort has been proposed. The passenger comfort was maximized through an appropriate choice of the weighting parameters of the controller. The parameters have been

selected by means of an optimization conducted with a Genetic Algorithm.

The method has been validated successfully in two different scenarios. The control strategy pointed out a good performance for both the lateral and longitudinal guidance. The speed profile was accurately followed while the lateral deviation is always within $0.1[m]$ and the relative yaw angle varied in the range ± 0.5 [deg]. Acceptable values of both the lateral and longitudinal accelerations were always kept. Consequently, the comfort evaluation was satisfactory in both scenarios. The equivalent acceleration a_{eq} always highlighted "not uncomfortable" condition while according to *MSDV*, the percentage of people who may experience nausea was below 5% in all the considered scenarios. The proposed design technique has highlighted easy applicability to different control strategies since good tracking and control performance was also observed in the architecture combining MPC and PID. Finally, the robustness analysis, when varying vehicle parameters from nominal values, demonstrated the effectiveness of the proposed method in a simulation environment. The promising results encourage the experimental validation of the method on a real vehicle.

Declaration of conflicting interests

The author(s) declared no potential conflicts of interest with respect to the research, authorship, and/or publication of this article.

Funding

The author(s) received no financial support for the research, authorship, and/or publication of this article.

ORCID iD

Sara Luciani https://orcid.org/0000-0002-5900-1409

References

1. Falcone P, Borrelli F, Asgari J, et al. Predictive active steering control for autonomous vehicle systems. *IEEE Transactions on Control Systems Technology* 2007; 15: 566–580.
2. Buratta V. *Esame delle proposte di legge recanti "Modifiche al codice della strada"*. 2019, p. 17.
3. On-Road Automated Driving (ORAD) Committee. Taxonomy and definitions for terms related to driving automation systems for on-road motor vehicles. *SAE Int* 2018; Vehicle El: 35.
4. Paden B, Cap M, Yong SZ, et al. A survey of motion planning and control techniques for self-driving urban vehicles. *IEEE Transactions on Control Systems Technology* 2016; 1: 33–55.
5. Coulter RC. Implementation of the pure pursuit path tracking algorithm. *Communication*. Epub ahead of print 1992. DOI: CMU-RI-TR-92-01.
6. Hoffmann GM, Tomlin CJ, Montemerlo M, et al. Autonomous automobile trajectory tracking for off-road driving: controller design, experimental validation and racing. In: *American control conference*, New York, NY, USA, 9–13 July 2007, pp. 2296–2301. New York: IEEE.
7. Dorum J, Utstumo T and Gravdahl JT. Experimental comparison of adaptive controllers for trajectory tracking in agricultural robotics. In: *2015 19th international conference on system theory, control and computing (ICSTCC) joint conference SINTES 19, SACCS 15, SIMSIS 19*, Cheile Gradistei, Romania, 14–16 October 2015, pp. 206–212. New York: IEEE.
8. Raffin A, Taragna M and Giorelli M. Adaptive longitudinal control of an autonomous vehicle with an approximate knowledge of its parameters. In: *11th international workshop on robot motion and control RoMoCo 2017 - work proceedings*, Wąsowo Palace, Poland, 3–5 July 2017, pp. 1–6. New York: IEEE.
9. Hima S, Glaser S, Chaibet A, et al. Controller design for trajectory tracking of autonomous passenger vehicles. In: *14th international IEEE conference on intelligent transportation systems (ITSC)*, Washington, DC, 5–7 October 2011, pp. 1459–1464. New York: IEEE.
10. Zhao P, Chen J, Song Y, et al. Design of a control system for an autonomous vehicle based on adaptive-PID. *Int J Adv Robot Syst* 2012; 9: 1–11.
11. Dai Y and Lee S-G. Perception, planning and control for self-driving system based on on-board sensors. *Adv Mech Eng* 2020; 12: 1–13.
12. Wan L, Su Y, Zhang H, et al. Neural adaptive sliding mode controller for unmanned surface vehicle steering system. *Adv Mech Eng* 2018; 10: 1–12.
13. Levinson J, Askeland J, Becker J, et al. Towards fully autonomous driving: systems and algorithms. In: *IEEE intelligent vehicles symposium (IV)*, Baden-Baden, Germany, 5–9 June 2011, pp. 163–168. New York: IEEE.
14. Marcano M, Matute JA, Lattarulo R, et al. Low speed longitudinal control algorithms for automated vehicles in simulation and real platforms. *Complexity* 2018; 2018: 7615123.
15. Feraco S, Bonfitto A, Amati N, et al. Combined lane keeping and longitudinal speed control for autonomous driving. In: *ASME 2019 international design engineering technical conferences and computers and information in engineering conference*, Anaheim, CA, 2019, vol. 3, pp. 1–8. New York: ASME.
16. Daoud MA, Osman M, Mehrez MW, et al. Path-following and adjustable driving behavior of autonomous vehicles using dual-objective nonlinear MPC. In: *2019 IEEE international conference of vehicular electronics and safety (ICVES)*, 2019, pp. 1–6, New York: IEEE.
17. Carvalho A, Gao Y, Gray A, et al. Predictive control of an autonomous ground vehicle using an iterative linearization approach. In: *16th International IEEE conference on intelligent transportation systems (ITSC 2013)*, The

Hague, Netherlands, 2013, pp. 2335–2340. New York: IEEE.
18. Yu H, Duan J, Taheri S, et al. A model predictive control approach combined unscented Kalman filter vehicle state estimation in intelligent vehicle trajectory tracking. *Adv Mech Eng* 2015; 7: 1–14.
19. Ren YY, Wang J, Zheng XL, et al. Research on multidimensional evaluation of tracking control strategies for self-driving vehicles. *Adv Mech Eng* 2020; 12: 1–15.
20. Faris WF, BenLahcene Z and Hasbullah F. Ride quality of passenger cars: an overview on the research trends. *Int J Veh Noise Vib* 2012; 8: 185–199.
21. Whitsitt S and Sprinkle J. A passenger comfort controller for an autonomous ground vehicle. In: *2012 IEEE 51st IEEE conference on decision and control (CDC)*, Maui, HI, 2013, pp. 3380–3385.
22. Mohseni F, Aslund J, Frisk E, et al. Fuel and comfort efficient cooperative control for autonomous vehicles. In: *2017 IEEE intelligent vehicles symposium (IV)*, Los Angeles, CA, 11–14 June 2017, pp. 1631–1636. New York: IEEE.
23. Du Y, Liu C and Li Y. Velocity control strategies to improve automated vehicle driving comfort. *IEEE Transactions on Control Systems Technology* 2018; 10: 8–18.
24. Eriksson J and Svensson L. *Tuning for ride quality in autonomous vehicle*. Dissertation, Uppsala University, Uppsala, 2015, p.61.
25. International Organization for Standardization. Mechanical vibration and shock: evaluation of human exposure to whole-body vibration. Part 1, general requirements - amendment1 ISO 2631-1: 1997/Amd 1: 2010. https://www.iso.org/standard/45604.html
26. Rajamani R. *Vehicle dynamics and control*. New York, NY: Springer, 2006.
27. Elbanhawi M, Simic M and Jazar R. In the passenger seat: investigating ride comfort measures in autonomous cars. *IEEE Transactions on Control Systems Technology* 2015; 7: 4–17.
28. Schmid C and Biegler LT. Quadratic programming methods for reduced hessian SQP. *Comput Chem Eng* 1994; 18: 817–832.
29. Bonfitto A, Tonoli A and Amati N. Viscoelastic dampers for rotors: modeling and validation at component and system level. *Appl Sci* 2017; 7: 1181.
30. Che H, Wu B, Yang J, et al. Speed sensorless sliding mode control of induction motor based on genetic algorithm optimization. *Meas Control (United Kingdom)* 2020; 53: 192–204.